Precise QCD predictions for the production of Higgs + jet final states

X. Chen [a], T. Gehrmann [b], E.W.N. Glover [a], M. Jaquier [b,*]

[a] *Institute for Particle Physics Phenomenology, Department of Physics, University of Durham, Durham, DH1 3LE, UK*
[b] *Department of Physics, University of Zürich, CH-8057 Zürich, Switzerland*

A B S T R A C T

We compute the cross section and differential distributions for the production of a Standard Model Higgs boson in association with a hadronic jet to next-to-next-to-leading order in quantum chromodynamics (QCD). In Higgs boson studies at the LHC, final states containing one jet are a dominant contribution to the total event rate, and their understanding is crucial for improved determinations of the Higgs boson properties. We observe substantial higher order corrections to transverse momentum spectra and rapidity distributions in Higgs-plus-one-jet final states. Their inclusion stabilises the residual theoretical uncertainty of the predictions around 9%, thereby providing important input to precision studies of the Higgs boson.

After the initial observation of a Standard Model-like Higgs boson at the CERN LHC [1,2], precision studies of the properties of the new particle is one of the primary objectives of the upcoming run at the LHC. Careful measurements of production and decay modes will enable searches for possible small deviations from the Standard Model formulation of the Higgs mechanism of electroweak symmetry breaking. The interpretation of these precision data relies on a close interplay between experimental measurements and theoretical calculations for Higgs boson signal and background processes.

To obtain reliable theoretical predictions for hadron collider observables, corrections from higher order processes in QCD need to be accounted for. For the most important Higgs boson production processes, impressive progress has been made in recent years, such that gluon fusion [3] and associated production [4] are described fully exclusively to next-to-next-to-leading order (NNLO) in QCD, and vector-boson-fusion [5] and associated production with top quarks [6] to next-to-leading order (NLO). For the gluon fusion process, which is the largest contribution to Higgs production at the LHC, NLO corrections have also been derived for Higgs boson production in association with up to three jets [7–9]. Recently, the first steps towards the fourth-order QCD corrections (N³LO) have been taken [10].

The number of jets produced in association with a Higgs boson candidate is a very important discriminator between different production modes, and is utilised in the optimization of signal-to-background ratios, for example through the application of jet vetoes [11]. For many Higgs boson studies, final states with $H + 0$ jets and $H + 1$ jet contribute roughly equal amounts to the total cross section. A comparable theoretical precision for both processes in the dominant gluon fusion production mode is therefore mandatory for precision studies and to resolve potential correlations between both samples [12,13]. While the $H + 0$ jets process is described to NNLO [3] accuracy, $H + 1$ jet production is known fully differentially only to NLO [7]. A first step towards the NNLO corrections for this process has been taken in [14] with the purely gluonic contribution to the total $H + 1$ jet cross section. This work has highlighted that NNLO contributions to $H + 1$ jet final states are of substantial numerical magnitude [14] and clearly called for a more differential description. In this letter, we report on a new calculation of the gluonic NNLO contributions to $H + 1$ jet production in gluon fusion, carried out in the form of a parton-level event generator that provides the corrections in a fully differential form, including the Higgs decay to two photons. An extension to different Higgs boson decay modes is feasible. As pointed out in Ref. [14], the gluonic process dominates over the other subprocesses including the potentially large quark–gluon channel. We note that the techniques employed here can be applied to these other contributions.

The NNLO corrections to Higgs + jet production in hadronic collisions receive contributions from the three types of parton-level processes: (a) the two-loop corrections to Higgs-plus-three-parton processes [15], (b) the one-loop corrections to Higgs-plus-four-parton processes [16] and (c) the tree-level Higgs-plus-five-parton processes [17]. Fig. 1 shows representative Feynman diagrams for
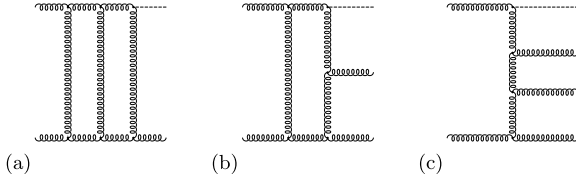
Fig. 1. Representative Feynman diagrams in the effective theory for (a) two-loop Higgs-plus-three-gluon amplitudes, (b) one-loop Higgs-plus-four-gluon amplitudes, and (c) tree-level Higgs-plus-five-gluon amplitudes.

each of the gluonic processes. The effective interaction between gluons and the Higgs boson is mediated by top quarks and is valid in the $m_t \to \infty$ limit. The ultraviolet renormalised matrix elements for these processes are integrated over the final state phase space appropriate to Higgs + jet final states. All three types of contributions are infrared-divergent, only their sum is finite. While infrared divergences from the virtual corrections are explicit in the one-loop and two-loop matrix elements, divergences from unresolved real radiation become explicit only after phase space integration. The divergences are usually regulated dimensionally, and different methods have been used for their extraction from the real radiation contributions. All these methods are based on a subtraction of divergent configurations, which are then integrated over the phase space and added to the virtual corrections to yield a finite result: sector decomposition [18], antenna subtraction [19], q_T-subtraction [20] and sector-improved residue subtraction [21] have all been applied successfully in the calculation of NNLO corrections to exclusive processes.

In this calculation we apply antenna subtraction, a method for the construction of real radiation subtraction terms based on so-called antenna functions, that each describe all infrared singular limits occurring in between two hard colour-ordered partons. For hadron-collider observables, either hard radiator can be in the initial or final state, and all unintegrated and integrated antenna functions were derived previously [22–25]. The gluonic cross-section is given by,

$$d\sigma_{gg,NNLO} = \int_{d\Phi_3} \left[d\sigma_{gg,NNLO}^{RR} - d\sigma_{gg,NNLO}^{S} \right]$$
$$+ \int_{d\Phi_2} \left[d\sigma_{gg,NNLO}^{RV} - d\sigma_{gg,NNLO}^{T} \right]$$
$$+ \int_{d\Phi_1} \left[d\sigma_{gg,NNLO}^{VV} - d\sigma_{gg,NNLO}^{U} \right], \tag{1}$$

where each of the square brackets is finite and well behaved in the infrared singular regions. The construction of the subtraction terms $d\sigma_{gg,NNLO}^{S,T,U}$ follows closely the NNLO subtraction terms for purely gluonic jet production [26].

Using the antenna subtraction method to cancel infrared divergent terms between different channels, we have implemented all purely gluonic subprocesses to Higgs-plus-jet production through to NNLO into a parton-level event generator. With this program, we can compute any infrared safe observable related to $H + j$ final states to NNLO accuracy. The Higgs decay to two photons is included, such that realistic event selection cuts on the photons can equally be applied once multiple differential distributions become available. Renormalization and factorization scales can be chosen on an event-by-event basis.

For our numerical computations, we use the NNPDF2.3 parton distribution functions [27] with the corresponding value of $\alpha_s(M_Z) = 0.118$ at NNLO, and $M_H = 125$ GeV. Default values for the factorization and renormalization scales are $\mu_F = \mu_R = M_H$,
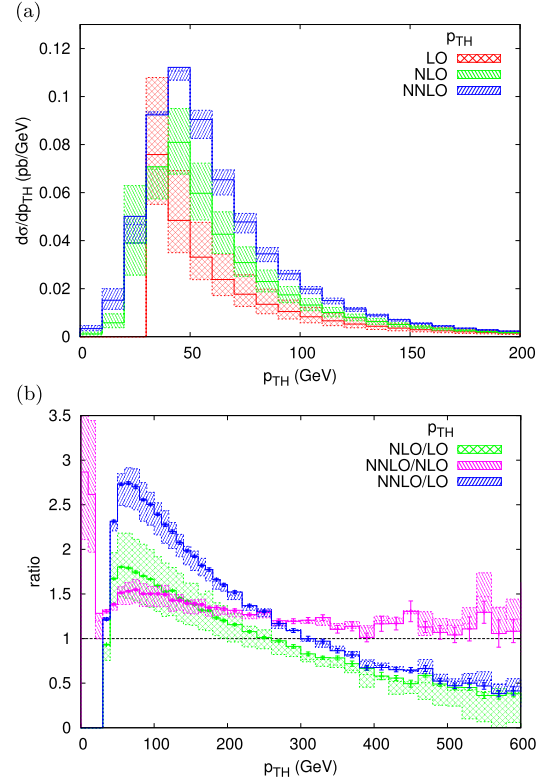

Fig. 2. (a) Transverse momentum distribution of the Higgs boson in inclusive $H + 1j$ production in pp collisions with $\sqrt{s} = 8$ TeV at LO, NLO, NNLO. (b) Ratios of different perturbative orders, NLO/LO, NNLO/LO and NNLO/NLO.

with theory errors estimated from the envelope of a variation to $M_H/2$ and $2M_H$. To compare with previously obtained results for the total cross section for purely gluonic $H + j$ production at $\sqrt{s} = 8$ TeV, we use the same cuts as in [14]: jets are reconstructed in the k_T algorithm with $R = 0.5$, and accepted if $p_T > 30$ GeV. With this, we obtain the total cross section at different perturbative orders as

$$\sigma_{LO} = 2.72^{+1.22}_{-0.78} \text{ pb},$$
$$\sigma_{NLO} = 4.38^{+0.76}_{-0.74} \text{ pb},$$
$$\sigma_{NNLO} = 6.34^{+0.28}_{-0.49} \text{ pb}, \tag{2}$$

in very good agreement with [14].

In our kinematical distributions and ratio plots, the error band describes the scale variation envelope as described above, where the denominator in the ratio plots is evaluated at fixed central scale, such that the band only reflects the variation of the numerator. Error bars on the distributions indicate the numerical integration errors on individual bins.

The transverse momentum distribution of the Higgs boson is particularly important for discriminating between different Higgs production modes. A first measurement has recently been presented by ATLAS [28], demonstrating the feasibility and future experimental prospects for this observable. It has been computed previously to NLO [7], combined with resummation to third logarithmic order (NNLL) [29]. In Fig. 2, we observe that the Higgs boson transverse momentum distribution receives sizable NNLO corrections throughout the whole range in p_T, which enhance the NLO cross section by a quasi-constant factor of about 1.4, slightly decreasing towards higher p_T. Using the same scale variations pattern as for the inclusive cross section above, we observe that the p_T distribution of the Higgs boson has a residual NNLO theory
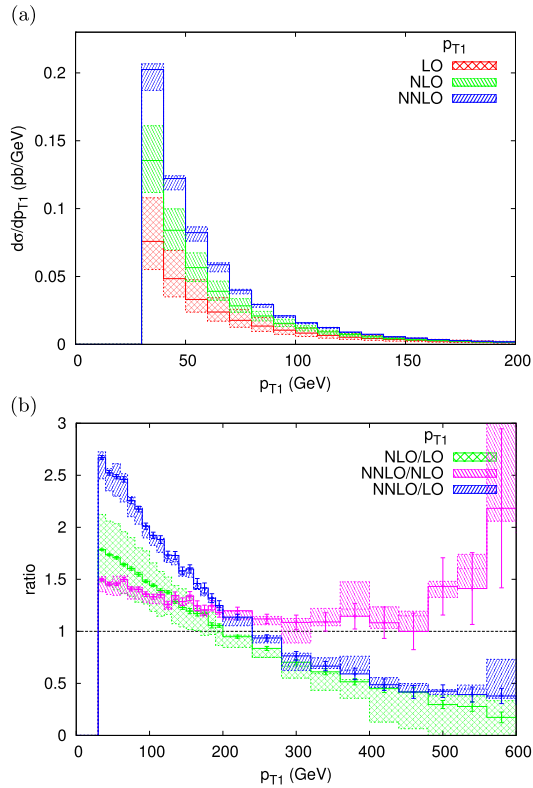
Fig. 3. (a) Transverse momentum distribution of the leading jet in inclusive $H + 1j$ production in pp collisions with $\sqrt{s} = 8$ TeV at LO, NLO, NNLO. (b) Ratios of different perturbative orders, NLO/LO, NNLO/LO and NNLO/NLO.

Fig. 4. (a) Rapidity distribution of the Higgs boson in inclusive $H + 1j$ production in pp collisions with $\sqrt{s} = 8$ TeV at LO, NLO, NNLO. (b) Ratios of different perturbative orders, NLO/LO, NNLO/LO and NNLO/NLO.

uncertainty ranging between 5% and 16%. At high values of p_T, the effective theory approximation used for the coupling of the Higgs boson to gluons breaks down, since the large momentum transfer in the process starts resolving the top quark loop. Consequently, one expects top quark mass effects for $p_T \gtrsim m_t$ to be more important than the higher order corrections in the effective theory. We extend the ratio plots, Figs. 2(b) and 3(b), to values well beyond $p_T \gtrsim m_t$ to illustrate the smooth behaviour and the qualitative tendency of the NNLO corrections in the effective theory.

We note that at leading order $p_{T,H}$ is kinematically forced to be equal to the transverse momentum of the jet, and is consequently larger than the transverse momentum cut on the jet. At higher orders, higher multiplicity final states are allowed and this kinematical restriction no longer applies. These kinematical situations often lead to instabilities in the perturbative expansion, with large corrections at each order. We observe that this is not the case here: NNLO corrections to the Higgs boson p_T distribution in $H + j$ events turn out to be moderate below the jet cut of $p_T = 30$ GeV. A similar pattern to the Higgs p_T distribution, is also observed for the leading jet, Fig. 3, which displays a slightly smaller scale uncertainty amounting up to 12%, and displays rising NNLO corrections for very large values of p_T, again likely beyond the applicability of the effective theory approximation.

The rapidity distribution of the Higgs boson and the leading jet are displayed in Figs. 4 and 5 respectively. In both cases, we observe that the NLO corrections are largest at central rapidity, while becoming moderate at larger rapidities, while the ratio NNLO/NLO remains rather constant throughout the rapidity range. The residual theory uncertainty at NNLO is quasi-constant for both distributions, and amounts to 9%. Both the transverse momentum and rapidity distributions highlight the fact that the NNLO corrections to $H + 1j$ production in the gluon-only channel substantially enhance
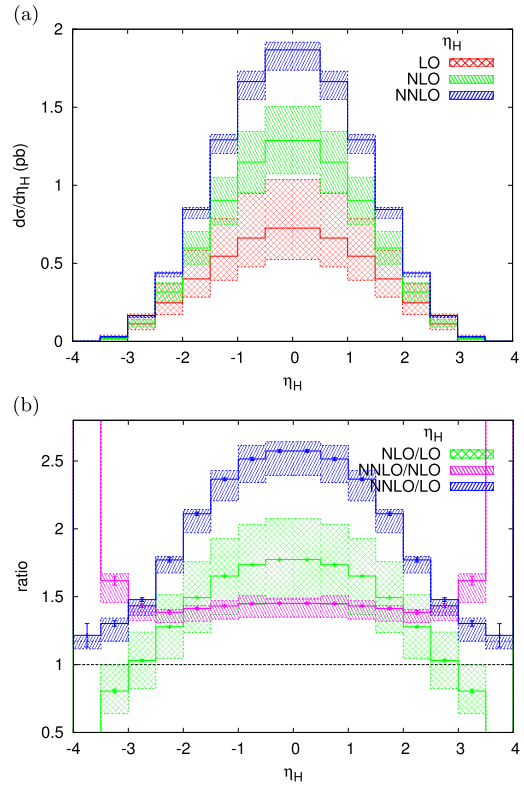

Fig. 5. (a) Rapidity distribution of the leading jet in inclusive $H + 1j$ production in pp collisions with $\sqrt{s} = 8$ TeV at LO, NLO, NNLO. (b) Ratios of different perturbative orders, NLO/LO, NNLO/LO and NNLO/NLO.
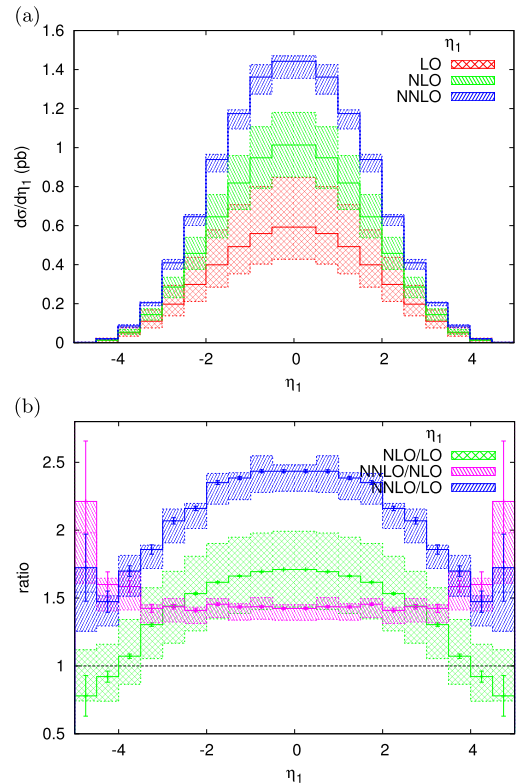
the normalization of NLO predictions, while not modifying the NLO shape, except around the production threshold.

In conclusion, we have described the first calculation of the fully differential $H + 1j$ cross sections at hadron colliders at NNLO in the strong coupling constant using a new parton-level event generator. We have considered the NNLO QCD corrections from the purely gluonic channel. Using the antenna subtraction scheme the explicit ϵ-poles in the dimension regularization parameter of one- and two-loop matrix elements entering this calculation are cancelled in analytic and local form against the ϵ-poles of the integrated antenna subtraction terms thereby enabling the computation of Higgs plus jet cross sections at hadron colliders at NNLO accuracy. The gluonic process yields the numerically largest contribution to $H + j$ final states, followed by the quark–gluon initiated and other subprocesses. However, the techniques employed here can be readily applied to the quark contributions. We observed that the transverse momentum and rapidity distributions of the Higgs boson and the leading jet receive substantial NNLO corrections. However, the shapes of the distributions do not change dramatically from NLO to NNLO, except around the production threshold in p_T.

For all of the observables considered here, we observed a reduction of the respective uncertainties in the theory prediction due to variations of the factorization and renormalization scales, resulting in a residual uncertainty of around 9% on the normalization of the distributions. We expect similar conclusions when including the processes involving quarks. Our calculation brings gluonic $H + j$ production to the same level of theory accuracy as inclusive H production, and will thus provide a crucial tool for precision studies of the Higgs boson in the upcoming data taking periods at the CERN LHC.

References

[1] G. Aad, et al., ATLAS Collaboration, Phys. Lett. B 716 (2012) 1, arXiv:1207.7214;
S. Chatrchyan, et al., CMS Collaboration, Phys. Lett. B 716 (2012) 30, arXiv:1207.7235.

[2] G. Aad, et al., ATLAS Collaboration, ATLAS-CONF-2014-009;
S. Chatrchyan, et al., CMS Collaboration, CMS-PAS-HIG-14-009;
V. Khachatryan, et al., CMS Collaboration, Phys. Lett. B 736 (2014) 64, arXiv:1405.3455.

[3] C. Anastasiou, K. Melnikov, F. Petriello, Nucl. Phys. B 724 (2005) 197, arXiv:hep-ph/0501130;
M. Grazzini, J. High Energy Phys. 0802 (2008) 043, arXiv:0801.3232.

[4] G. Ferrera, M. Grazzini, F. Tramontano, Phys. Rev. Lett. 107 (2011) 152003, arXiv:1107.1164;
G. Ferrera, M. Grazzini, F. Tramontano, J. High Energy Phys. 1404 (2014) 039, arXiv:1312.1669.

[5] T. Figy, C. Oleari, D. Zeppenfeld, Phys. Rev. D 68 (2003) 073005, arXiv:hep-ph/0306109;
K. Arnold, et al., Comput. Phys. Commun. 180 (2009) 1661, arXiv:0811.4559;
F. Campanario, T.M. Figy, S. Plätzer, M. Sjödahl, Phys. Rev. Lett. 111 (2013) 211802, arXiv:1308.2932.

[6] W. Beenakker, S. Dittmaier, M. Kramer, B. Plumper, M. Spira, P.M. Zerwas, Nucl. Phys. B 653 (2003) 151, arXiv:hep-ph/0211352;
S. Dawson, C. Jackson, L.H. Orr, L. Reina, D. Wackeroth, Phys. Rev. D 68 (2003) 034022, arXiv:hep-ph/0305087;
R. Frederix, S. Frixione, V. Hirschi, F. Maltoni, R. Pittau, P. Torrielli, Phys. Lett. B 701 (2011) 427, arXiv:1104.5613.

[7] D. de Florian, M. Grazzini, Z. Kunszt, Phys. Rev. Lett. 82 (1999) 5209, arXiv:hep-ph/9902483;
V. Ravindran, J. Smith, W.L. Van Neerven, Nucl. Phys. B 634 (2002) 247, arXiv:hep-ph/0201114.

[8] J.M. Campbell, R.K. Ellis, G. Zanderighi, J. High Energy Phys. 0610 (2006) 028, arXiv:hep-ph/0608194;
J.M. Campbell, R.K. Ellis, C. Williams, Phys. Rev. D 81 (2010) 074023, arXiv:1001.4495;
H. van Deurzen, N. Greiner, G. Luisoni, P. Mastrolia, E. Mirabella, G. Ossola, T. Peraro, J.F. von Soden-Fraunhofen, et al., Phys. Lett. B 721 (2013) 74, arXiv:1301.0493.

[9] G. Cullen, H. van Deurzen, N. Greiner, G. Luisoni, P. Mastrolia, E. Mirabella, G. Ossola, T. Peraro, F. Tramontano, Phys. Rev. Lett. 111 (2013) 131801, arXiv:1307.4737.

[10] C. Anastasiou, C. Duhr, F. Dulat, E. Furlan, T. Gehrmann, F. Herzog, B. Mistlberger, Phys. Lett. B 737 (2014) 325, arXiv:1403.4616.

[11] S. Catani, D. de Florian, M. Grazzini, J. High Energy Phys. 0201 (2002) 015, arXiv:hep-ph/0111164.

[12] I.W. Stewart, F.J. Tackmann, Phys. Rev. D 85 (2012) 034011, arXiv:1107.2117.

[13] E. Gerwick, T. Plehn, S. Schumann, Phys. Rev. Lett. 108 (2012) 032003, arXiv:1108.3335.

[14] R. Boughezal, F. Caola, K. Melnikov, F. Petriello, M. Schulze, J. High Energy Phys. 1306 (2013) 072, arXiv:1302.6216.

[15] T. Gehrmann, M. Jaquier, E.W.N. Glover, A. Koukoutsakis, J. High Energy Phys. 1202 (2012) 056, arXiv:1112.3554.

[16] L.J. Dixon, Y. Sofianatos, J. High Energy Phys. 0908 (2009) 058, arXiv:0906.0008;
S. Badger, E.W.N. Glover, P. Mastrolia, C. Williams, J. High Energy Phys. 1001 (2010) 036, arXiv:0909.4475;
S. Badger, J.M. Campbell, R.K. Ellis, C. Williams, J. High Energy Phys. 0912 (2009) 035, arXiv:0910.4481.

[17] V. Del Duca, A. Frizzo, F. Maltoni, J. High Energy Phys. 0405 (2004) 064, arXiv:hep-ph/0404013;
L.J. Dixon, E.W.N. Glover, V.V. Khoze, J. High Energy Phys. 0412 (2004) 015, arXiv:hep-th/0411092;
S.D. Badger, E.W.N. Glover, V.V. Khoze, J. High Energy Phys. 0503 (2005) 023, arXiv:hep-th/0412275.

[18] T. Binoth, G. Heinrich, Nucl. Phys. B 693 (2004) 134, arXiv:hep-ph/0402265;
C. Anastasiou, K. Melnikov, F. Petriello, Phys. Rev. D 69 (2004) 076010, arXiv:hep-ph/0311311.

[19] A. Gehrmann-De Ridder, T. Gehrmann, E.W.N. Glover, J. High Energy Phys. 0509 (2005) 056, arXiv:hep-ph/0505111;
A. Gehrmann-De Ridder, T. Gehrmann, E.W.N. Glover, Phys. Lett. B 612 (2005) 49, arXiv:hep-ph/0502110;
A. Gehrmann-De Ridder, T. Gehrmann, E.W.N. Glover, Phys. Lett. B 612 (2005) 36, arXiv:hep-ph/0501291.

[20] S. Catani, M. Grazzini, Phys. Rev. Lett. 98 (2007) 222002, arXiv:hep-ph/0703012.

[21] M. Czakon, Phys. Lett. B 693 (2010) 259, arXiv:1005.0274.

[22] A. Daleo, T. Gehrmann, D. Maitre, J. High Energy Phys. 0704 (2007) 016, arXiv:hep-ph/0612257.

[23] A. Daleo, A. Gehrmann-De Ridder, T. Gehrmann, G. Luisoni, J. High Energy Phys. 1001 (2010) 118, arXiv:0912.0374.

[24] T. Gehrmann, P.F. Monni, J. High Energy Phys. 1112 (2011) 049, arXiv:1107.4037.

[25] R. Boughezal, A. Gehrmann-De Ridder, M. Ritzmann, J. High Energy Phys. 1102 (2011) 098, arXiv:1011.6631;
A. Gehrmann-De Ridder, T. Gehrmann, M. Ritzmann, J. High Energy Phys. 1210 (2012) 047, arXiv:1207.5779.

[26] E.W.N. Glover, J. Pires, J. High Energy Phys. 1006 (2010) 096, arXiv:1003.2824;
A. Gehrmann-De Ridder, E.W.N. Glover, J. Pires, J. High Energy Phys. 1202 (2012) 141, arXiv:1112.3613;
A. Gehrmann-De Ridder, T. Gehrmann, E.W.N. Glover, J. Pires, J. High Energy Phys. 1302 (2013) 026, arXiv:1211.2710;
A. Gehrmann-De Ridder, T. Gehrmann, E.W.N. Glover, J. Pires, Phys. Rev. Lett. 110 (2013) 162003, arXiv:1301.7310.

[27] R.D. Ball, et al., Nucl. Phys. B 867 (2013) 244, arXiv:1207.1303.

[28] G. Aad, et al., ATLAS Collaboration, J. High Energy Phys. 1409 (2014) 112, arXiv:1407.4222.

[29] C. Balazs, C.P. Yuan, Phys. Lett. B 478 (2000) 192, arXiv:hep-ph/0001103;
G. Bozzi, S. Catani, D. de Florian, M. Grazzini, Nucl. Phys. B 737 (2006) 73, arXiv:hep-ph/0508068;
V. Ahrens, T. Becher, M. Neubert, L.L. Yang, Eur. Phys. J. C 62 (2009) 333, arXiv:0809.4283;
D. de Florian, G. Ferrera, M. Grazzini, D. Tommasini, J. High Energy Phys. 1111 (2011) 064, arXiv:1109.2109;
D. de Florian, G. Ferrera, M. Grazzini, D. Tommasini, J. High Energy Phys. 1206 (2012) 132, arXiv:1203.6321.